Monatomic-Molecular Transition in Expanded Rubidium

W.-C. Pilgrim,[1] M. Ross,[1,2] L. H. Yang,[2] and F. Hensel[1]
[1]*Institute of Physical Chemistry and Materials Science Centre, Philipps-University of Marburg, 35032 Marburg, Germany*
[2]*Lawrence Livermore National Laboratory, University of California, Livermore, California 944551*
(Received 6 January 1997)

$S(Q, \omega)$ for liquid rubidium measured along the liquid vapor coexistence line exhibits monatomic behavior from normal density down to twice the critical density. At this density we observe excitations characteristic of a harmonic oscillator. We interpret this as evidence for the passage of the fluid from a monatomic to a molecular state. First principle total energy calculations for lattices of ribidium at 0 K predict that expansion favors spin pairing and leads to a lattice of dimers with an increase in vibron energy with decreasing density. The excellent agreement of the calculated vibron energy with the experimental result provides theoretical support for the appearance of molecules. [S0031-9007(97)03149-9]

PACS numbers: 61.25.Mv, 61.12.Ex, 64.70.Ja, 71.30.+h

Liquid alkali metals at high densities close to their triple points can be regarded as monatomic fluids, where each atom contributes one single electron to a half-filled conduction band [1]. This view is consistent with several experimental observations: The dynamic structure factor $S(Q, \omega)$ for liquid rubidium measured at conditions close to the melting point exhibits distinct collective excitations at a high wave vector [2] typical for dense metallic fluids. The dispersion relation of these excitations is in accord with the result from computer simulations employing an interatomic pseudopotential typical for monatomic metals [3].

Measurements of the static structure factor $S(Q)$ for fluid rubidium and cesium [4,5], carried out along the liquid vapor coexistence line for several densities between the melting point and the critical point, are consistent with this view. The main structural effect of the density decrease with increasing temperature is a reduction in the average number of nearest neighbors within the first coordination shell around an atom, while the mean interparticle distance remains nearly unchanged. This behavior changes dramatically if the metals are evaporated to the dilute gas phase close to their triple points. Under these conditions, alkali metal vapors behave like typical insulators with electrical conductivities less than $10^{-5}\ \Omega^{-1}\,\mathrm{cm}^{-1}$ [6]. Measurements of optical [7,8] and magnetic [9] properties and of equation of state data [8,10], as a function of density indicate that molecular aggregates such as dimers or trimers do exist in the gas phase. As the vapor is compressed along the coexistence line the experimental results indicate an increase in concentration of the molecular species to about 25% at conditions close to the critical point [9]. Resent theoretical considerations of these data reach a similar conclusion [11]. The question to emerge from these findings is, up to what density can the pairing mechanism present in the vapor survive the passage from the dilute vapor to the dense liquid [1,12].

Recently, we were able to extend our measurements of the dynamic structure factor $S(Q, \omega)$ for liquid rubidium to densities as low as twice the critical density, where deviations from the metallic behavior are already significant [13]. The liquid was expanded along the coexistence line toward the critical point ($T_c = 2017$ K and $\rho_c = 0.29\ \mathrm{g/cm}^3$ [14]) by simultaneously increasing the temperature and pressure. Up to moderate liquid densities of about three times the critical density ($0.83\ \mathrm{g/cm}^3$), the results are in accord with molecular dynamics calculations [15] employing effective pair potentials derived by pseudopotential theory, typical for monatomic metals.

At the lowest density measured ($0.61\ \mathrm{g/cm}^3$, i.e., about two times the critical density), drastic changes in $S(Q, \omega)$ are observed. A well-defined excitation peak appears near $\hbar\omega = 3.2$ meV with the maximum intensity at a momentum transfer near $1\ \text{Å}^{-1}$. Its size is clearly outside the experimental error which does not exceed 5% of the intensity in $S(Q, \omega)$. This observation was interpreted as an optic-type mode [7] in which two atoms tend to move in opposite directions. The Q dependence of the peak intensity is qualitatively consistent with a model assuming the existence of diatomic harmonic oscillators in the liquid [13,16]. As an example, the results, expressed as $S(Q, \omega)$ for $1.0\ \text{Å}^{-1}$, and in terms of the longitudinal current correlation function $J_1(Q, \omega) = (\omega^2/Q^2)S(Q, \omega)$ for $Q = 1.3\ \text{Å}^{-1}$, are given in Fig. 1 for the experimental conditions investigated in this experiment. At these values of momentum transfer, the excitations are best observable due to the intensity dependence of the excitation [7] and the shape of the coherent dynamic structure factor. The drastic changes in shape occurring when the lowest density is reached at 1873 K are apparent in both $S(Q, \omega)$ and $J_1(Q, \omega)$. The curves exhibit excitation peaks clearly larger than the statistical error. In $S(Q, \omega)$ the peak is centered around 3.2 meV, while in $J_1(Q, \omega)$ the peaks can be identified as resulting from excitations at 3.2 meV with higher harmonics at 6.4 and 9.6 meV slightly shifted to higher frequencies due to the ω^2 term in $J_1(Q, \omega)$.

Despite the high thermal energy at 1873 K, the observed peaks in $S(Q, \omega)$ and in $J_1(Q, \omega)$ reveal

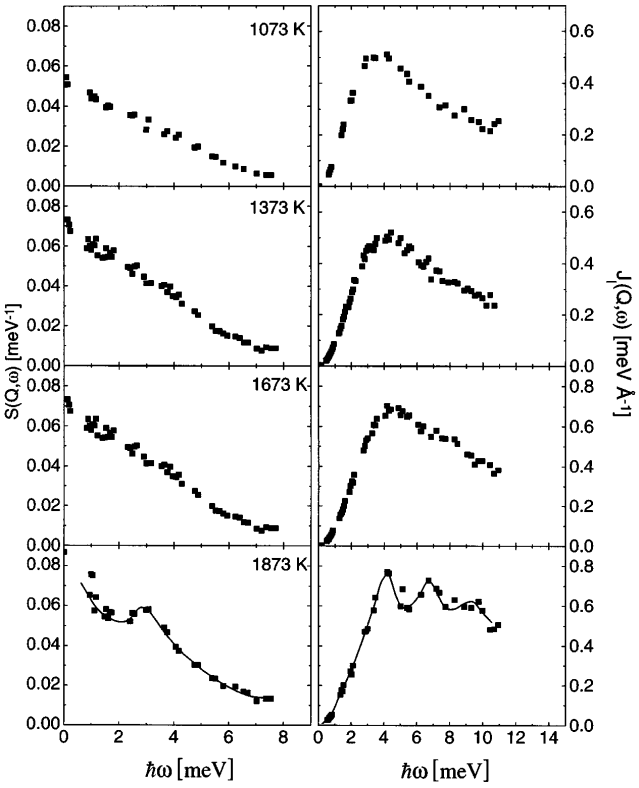

FIG. 1. Experimentally determined scattering laws $S(Q,\omega)$ at $Q = 1.0$ Å^{-1} and current correlation functions $J_1(Q,\omega) = (\omega^2/Q^2)S(Q,\omega)$ at $Q = 1.3$ Å^{-1} for four different liquid densities, measured along the liquid vapor coexistence curve: 1073 K, $\rho = 1.13$ g/cm^3; 1373 K, 0.98 g/cm^3; 1673 K, 0.87 g/cm^3; 1873 K, 0.61 g/cm^3. The lines at 1873 K are just a guide for the eye.

surprisingly small linewidths. This is a common observation in neutron spectroscopy. For a freely moving molecule executing harmonic oscillations relative to its center of mass, the linewidth of an excitation is proportional to $\sqrt{k_B T E_R}$, where $E_R = \hbar^2 Q^2/2M_{\mathrm{mol}}$ represents the recoil energy and M_{mol} is the mass of the molecule [16]. At 1873 K this gives a value of 1.83 meV which is comparable with the linewidth found in $S(Q,\omega)$.

In order to gain some insight on a microscopic level for the appearance of a vibron in expanded rubidium, we have undertaken exploratory calculations for the total energy of expanded lattices of monoatomic Rb and Rb_2 dimers using density functional theory (DFT) in the local density approximation (LDA) [17]. DFT is a first principle quantum mechanical method for calculating total energies with the exchange and correlation terms written in terms of the local electron density (LDA). The computational method used here is the same as that reported previously for a similar set of calculations made for lattices of Cs and Cs_2 [18].

Calculations were made for a system of Rb atoms in a body-centered lattice (bcc) and for diatomic molecules in a simple cubic lattice (sc). To create the diatomic solid the two atoms in the bcc unit cell were moved towards each other, forming a simple cubic lattice. The dimer bond length in the molecular lattice was varied to minimize the total energy. In Fig. 2, the difference in calculated total energy (per two atoms) between the Rb_2 and Rb static lattices is plotted versus density on a scale for which the energy of the bcc lattice is zero. Below a density of 0.9 g/cm^3 the sc-Rb_2 lattice has the lowest energy.

The vibron energy ($h\nu$) and dissociation energy (D_e) were obtained by displacing the bond length from its equilibrium value R_0 and calculating the change in energy $E(R - R_0)$. These data were then fitted to a Morse potential [19]. As an illustration, Fig. 3 shows $E(R - R_0)$ plotted versus $R - R_0$ at a density of 0.62 g/cm^3. The values of $h\nu$ and D_e obtained from the Morse fit are plotted versus density in Figs. 4 and 5. The points in the gas at $\rho = 0$ g/cm^3 [20] connect smoothly with the calculations at higher density. Shown in Fig. 4 is the experimental data point, at $\rho = 0.61$ g/cm^3 and $h\nu = 3.2$ meV, which is in remarkably good agreement with the present calculations.

Our calculations predict that the vibron and dissociation energy decrease with increasing density from their gas phase value to zero near 0.9 g/cm^3. Such a decrease in the vibron energy with increasing density is now a well-established feature found in optical studies on solid molecular hydrogen [21] and nitrogen [22]. This decrease is believed to be associated with the transfer of electron charge towards neighboring molecules, leading to a softening of the molecular bond and the formation of a monatomic state. With increasing density the intramolecular bond distance R_0 increases steadily from 4.17 Å in the gas phase [23] to 4.40 Å near the experimental

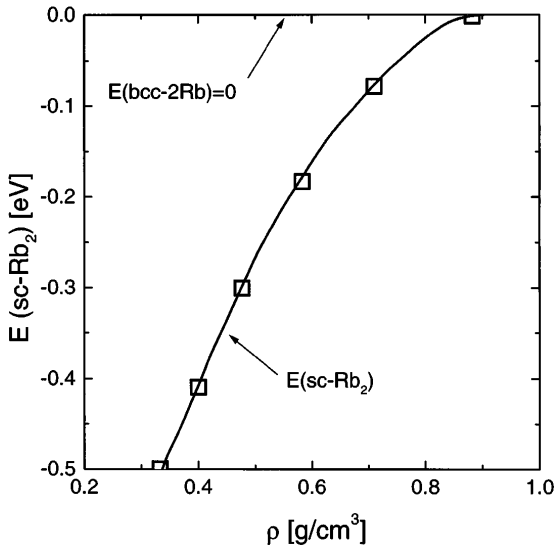

FIG. 2. The difference in calculated total energy E (per two atoms) between the Rb_2 and Rb static lattices as a function of density. On the scale shown, the energy of the Rb-bcc lattice is set to zero. The line is a smooth fit to the data.

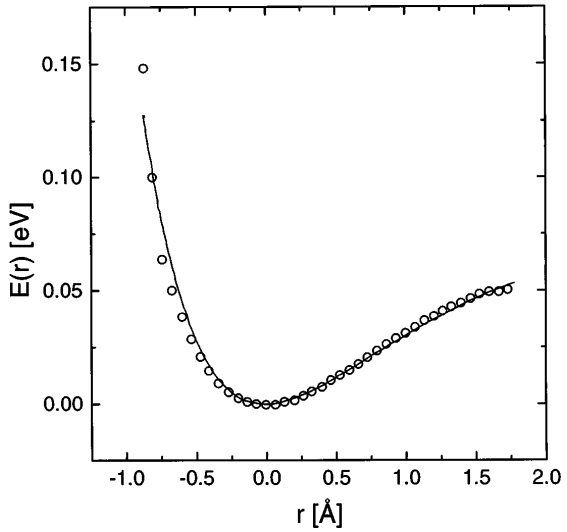

FIG. 3. Potential vibron energy $E(r)$ for the Rb_2 dimer as a function of bond length displacement $r = R - R_0$ for $\rho = 0.62$ g/cm^3. Open circles are calculated values; the solid line is a fit to a Morse potential.

density of 0.61 g/cm^3. Further compression of the fluid to about 0.87 g/cm^3, which is close to the density where the vibron frequency goes to zero, leads to an elongation of the bond to 5.52 Å. Evidence for this feature is also seen in Fig. 3 by the anharmonic character of the vibron in extension. In the case of hydrogen and nitrogen, the dissociation energies are nearly an order of magnitude larger than for the alkali metals, and these molecules are believed to metallize in the solid at pressures of several megabar. In contrast, the dimerization of Rb occurs in the expanded state at a low pressure and is only stabilized in the fluid at a temperature near 1700 K.

The effect of temperature on the composition is an important concern in deciding whether the predicted concentration of molecules in the liquid is sufficiently high to be observable in neutron scattering experiments. At the conditions of interest along the liquid vapor coexistence line, molecular dissociation will be favored by the high temperatures, in the range of 1700 to 2000 K. The fraction of molecules present in the liquid was calculated with the mass action equation [24,25] for an equilibrium mixture of atoms and dimers using the values of $h\nu$ and D_e from Figs. 4 and 5. The vibrational partition function was calculated by summing over all states of the Morse oscillator. The temperature at each density along the liquid-vapor curve was obtained from the experimental results of Jüngst *et al.* [14]. Plotted in Fig. 6 are the calculated fractions of Rb_2. Near a density of 0.9 g/cm^3 the fraction is zero and increases to a maximum value of about 38% at about 0.5 g/cm^3. The amount of Rb_2 then decreases at lower density due to the effect of entropy. At the experimental density (0.61 g/cm^3), the calculations predict a concentration of about 25% Rb_2 with a dissociation energy of 90 meV, which is large enough to account for the presence of three vibrational energy levels. In the absence of theoretical modeling we cannot precisely attach significance to the apparent result that the dimer fraction is highest at a density greater than the critical density. However, it has been shown that a compositional asymmetry along the liquid vapor equilibrium can be the origin of the

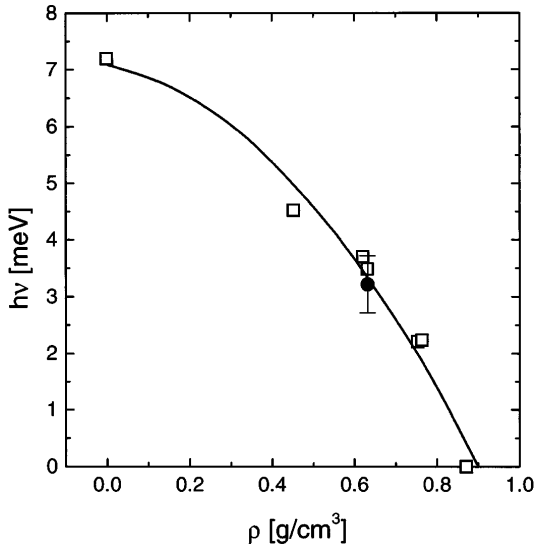

FIG. 4. Variation of the vibron energy $h\nu$ for Rb_2 with liquid density obtained from fitting the calculated values $E(r)$ to a Morse potential at each density. Included is the experimentally determined value at $\rho = 0.61$ g/cm^3. Open squares are calculated values; the solid circle represents the experimental result. The line is a smooth fit to the calculated data.

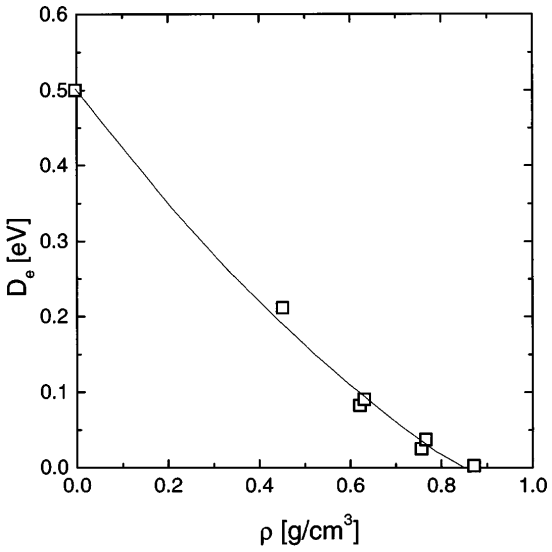

FIG. 5. Variation of the dissociation energy D_e for Rb_2 with liquid density obtained from fitting the calculated values $E(r)$ to a Morse potential at each density. The line is a smooth fit to the data.

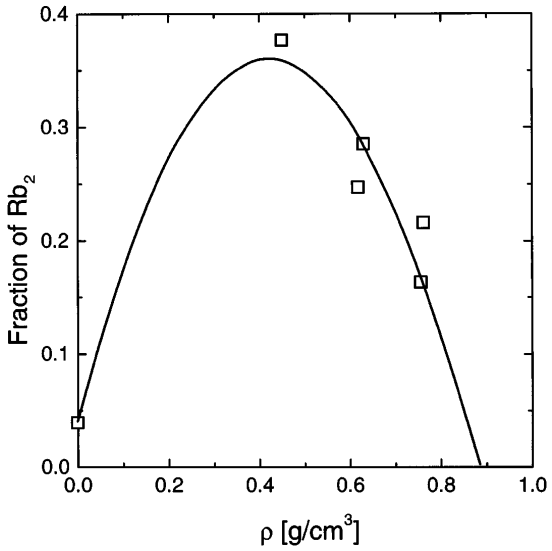

FIG. 6. Calculation of the dimer fraction in liquid rubidium for the considered densities, using the mass-cation law and values for $h\nu$ and D_e from the Morse potential fits. The partition function was calculated by summing over all states of the Morse oscillator. The line is a smooth fit to the data.

breakdown of the "law of rectilinear diameter" which is observed experimentally in expanded Rb and Cs [26].

In an alternative approach to the expanded metal vapor, Redmer and Warren [11] applied a plasma model to a partially dissociated and ionized gas of expanded ribidium and cesium. For rubidium they found that the highest density at which dimers appear is 0.8 g/cm^3, and they predict a dimer concentration of about 25% near the critical density. These results are in general agreement with our results.

M.R. gratefully acknowledges an Alexander von Humboldt Foundation Award for partial support of this work. L.H.Y. was supported at Lawrence Livermore National Laboratory by the U.S. Department of Energy under Contract No. W-31-109-ENG-38.

[1] N. W. Ashcroft, Nuovo Cimento D **12**, 597 (1990).
[2] J. R. D. Copley and J. M. Rowe, Phys. Rev. Lett. **32**, 49 (1974).
[3] A. Rahman, Phys. Rev. Lett. **32**, 52 (1974).
[4] G. Franz, W. Freyland, W. Gläser, F. Hensel, and E. Schneider, *Proceedings of the 4th International Conference on Liquid and Amorphous Metals* [J. Phys. Coll. **41**, 194 (1980)].
[5] R. Winter, T. Bodensteiner, W. Gläser, and F. Hensel, Ber. Bunsenges. Phys. Chem. **91**, 1327 (1987).
[6] A. A. Borzhievskii, V. A. Sechenov, and V. I. Khorunzhenko, Teplofiz. Vys. Temp. **26**, 722 (1988) [High Temp. **26**, 551 (1988)].
[7] W.-C. Pilgrim, R. Winter, and F. Hensel, J. Phys. Condens. Matter **5**, B183 (1993).
[8] F. Hensel and G. F. Hohl, Rev. High Pressure Sci. Technol. **3**, 163 (1994).
[9] W. Freyland, Phys. Rev. B **20**, 5104 (1979).
[10] C. T. Ewing, J. P. Stone, J. R. Spann, and R. R. Miller, J. Phys. Chem. **71**, 473 (1967).
[11] R. Redmer and W. W. Warren, Phys. Rev. B **48**, 14 892 (1993).
[12] N. H. March and M. P. Tosi, Adv. Phys. **44**, 299 (1995).
[13] W.-C. Pilgrim, Ph.D. thesis, Philipps-University, Marburg, 1992 (unpublished).
[14] S. Jüngst, B. Knuth, and F. Hensel, Phys. Rev. Lett. **55**, 2160 (1985).
[15] K. Hoshino, H. Ugawa, and M. Watabe, J. Phys. Soc. Jpn. **61**, 2182 (1992).
[16] S. W. Lovesey, *Theory of Neutron Scattering from Condensed Matter* (Clarendon, Oxford, 1984), Vol. 1.
[17] R. O. Jones and O. Gunnarson, Rev. Mod. Phys. **61**, 689 (1989).
[18] M. Ross, L. Yang, B. Dahling, and N. W. Winter, Z. Phys. Chem. **184**, 65 (1994).
[19] P. M. Morse, Phys. Rev. **34**, 57 (1929).
[20] M. Krauss and W. J. Stevens, J. Chem. Phys. **93**, 4236 (1990).
[21] H. K. Mao and R. J. Hemley, Rev. Mod. Phys. **66**, 671 (1994).
[22] R. Reichlin, D. Schiferl, S. Martin, C. Vanderborgh, and R. L. Mills, Phys. Rev. Lett. **55**, 1464 (1985).
[23] G. Höning, M. Czajkowski, M. Stock, and W. Demtröder, J. Chem. Phys. **71**, 2138 (1979).
[24] T. L. Hill, *An Introduction to Statistical Mechanics* (Addison-Wesley, Reading, MA, 1960).
[25] M. Ross, J. Chem. Phys. **86**, 7110 (1987).
[26] M. Ross and F. Hensel, J. Phys. Condens. Matter **8**, 1909 (1996).